JOURNAL OF SOLID STATE CHEMISTRY 98, 48–58 (1992)

A Monoclinic Form of the Seventh Member of the Tubular Oxides $(Bi_{2+x}Sr_{2-x}CuO_6)_nSr_{8-x'}Cu_6O_{16+y}$

M. T. CALDES,* M. HERVIEU, A. FUERTES,* AND B. RAVEAU

*Laboratoire de Cristallographie et Sciences des Matériaux, ISMRa, Bd du Maréchal Juin, 14050 Caen Cedex, France; and *Institut de Ciencias de Materiales, Campus UAB, 08193 Bellaterra, Barcelona, Spain*

Received July 15, 1991; in revised form October 23, 1991

A new monoclinic phase of the Bi–Sr–Cu–O system has been observed by X-ray and electron diffraction techniques in samples of the $n = 7$ tubular phases; the cell parameters are close to $a \approx a_p\sqrt{2} \approx 5.4$ Å, $b \approx 24.7$ Å, $c = 24.65$ Å, and $\alpha \approx 96°$, B centered. The high resolution electron microscopy study allowed a model to be proposed for this new phase. The structure is directly related to the orthorhombic tubular phases by a mechanism of shifting of the [(Bi, Sr)O] layers; it results in a double intergrowth along **b** and **c** of orthorhombic and monoclinic members. The mechanism is compared to those observed in the 2201 superconductor oxides. © 1992 Academic Press, Inc.

Introduction

After the discovery of the oxide $Bi_4Sr_8Cu_5O_{19+x}$ (*1*, *2*), a new family of tubular oxides with general formula $(Bi_{2+x}Sr_{2-x}CuO_6)_nSr_{8-x'}Cu_6O_{16+y}$ has been isolated and characterized for $n = 4$, 5, 6, and 7 (*3*). The different members of this series exhibit an orthorhombic symmetry and can be described as an intergrowth of $Bi_2Sr_2CuO_6$ ribbons, n octahedra wide, with an original layer $[Sr_8Cu_6O_{16}]_\infty$ related to the perovskite structure. The close relationships between these tubular phases and the layered superconductor $Bi_2Sr_2CuO_6$ (*4*, *5*) suggest a complex crystal chemistry. In fact, the real composition of the latter oxide is not perfectly known (*6–14*) but most of the authors agree with a strontium deficiency, and different formulations have been proposed for solid solutions, such as $Bi_2Sr_{2-x}CuO_{6-y}$ with $0.1 \leq x \leq 0.5$ (*10*) or $Bi_{2+x}Sr_{2-x}Cu_{1+y}O_{6+\delta}$ with $0.1 < x < 0.6$ and $y \approx x/4$ (*9*, *14*). It crystallizes in an orthorhombic subcell and exhibits a systematic modulation leading to a monoclinic cell. Near the composition of the modulated form, another form called "collapsed phase," with a monoclinic unit cell ($a = 24.47$ Å; $b = 5.42$ Å; $c = 21.96$ Å; $\beta = 105.4°$), was found (*8–13*), probably corresponding to the composition $Bi_{17}Sr_{16}Cu_7O_x$ (*9*). According to Takano and co-workers (*9*), the arrangement of the cations in the "collapsed" phase is closely related to that observed in the 2201 superconductor. This suggests that small variations of cationic molar ratios can involve structural changes in the orthorhombic tubular phases. We report here on a monoclinic form of the seventh member of the tubular family and on its structural relationships with the orthorhombic form and with the 2201-related oxides.

0022-4596/92 $5.00

Experimental

As previously reported (*1, 2*), the samples were prepared following two methods: the starting mixtures were either Bi_2O_3, $SrCO_3$ and CuO or "2201" as precursor with Sr_2CuO_3 and CuO. They were heated at temperatures ranging from 750 to 880°C in air. The samples were characterized by X-ray diffraction with a Philips diffractometer using Cu$K\alpha$ radiation. However, the powder patterns were often too complex, especially for the high n values, and an electron diffraction (E.D.) investigation was systematically carried out in order to identify the different phases. These studies were performed with a JEOL 120 CX microscope fitted with a side entry goniometer (±60°) and a JEOL 200CX electron microscope fitted with a double tilt goniometer (±10°).

Structural recall. The general formulation $(Bi_2Sr_2CuO_6)_n \cdot Sr_{8-x}Cu_6O_{16+y}$ expresses the mechanism which governs the formation of the orthorhombic tubular phases (*1, 3*). Their structure can be described from the intergrowth, along **b**, of n $[Bi_2Sr_2CuO_6]$ slices with an original layer, $[Sr_8Cu_6O_{16+y}]$, related to the perovskite structure. The idealized structure of the orthorhombic $n = 4$ tubular oxide is shown as example in Fig. 1: the 2201-type slices are labeled S_{2201} and the perovskite related pillars $[Sr_8Cu_6O_{16}]_\infty$ are labeled P. Pure phases have been isolated for $n = 4$ to 7.

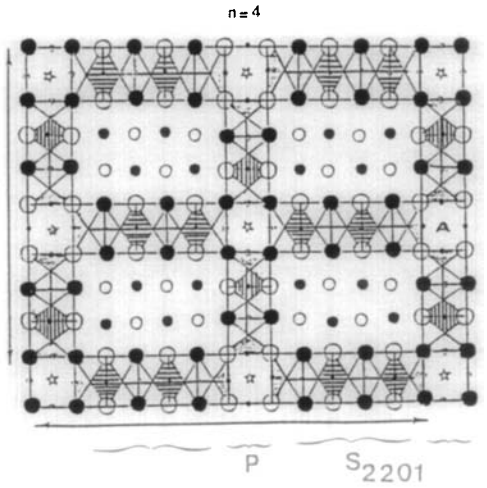

FIG. 1. Idealized drawing of the structure of $Bi_4Sr_8Cu_5O_{19+x}$, member $n = 4$ of the $(Bi_2Sr_2CuO_6)_n(Sr_{8-x}Cu_6O_{16+y})$ family. The projection direction is [100]. The open and black circles correspond to the cation positions with $x = 0$ or $x \frac{1}{2}$. The oxygen atoms in the copper layers are at $x = \frac{1}{4}$ and $x = \frac{3}{4}$; the copper octahedra are drawn, open or hatched in accordance with the x value of copper atom. The site labeled with a star corresponds to an oxygen atom which appears as highly disordered and probably deficient (*2*).

Results and Discussion

Synthesis

As previously shown (*3*) the orthorhombic tubular-7 oxide, $(Bi_{2+x}Sr_{2-x}CuO_6)_7 \cdot Sr_{8-x'}Cu_6O_{16}$ was obtained for the nominal cation ratio Bi/Sr/Cu of 13.0/19.5/13 by heating the starting mixture at 800°C for 96 hr in air; as previously noted, this composition is slightly Bi- and Sr-deficient with regard to the theoretical one (14/22/13).

Taking into account the fact that in the case of the 2201 modulated form, the formation of a new phase, the monoclinic "collapsed" phase, is favored by an excess of strontium (and Bi), we have investigated, for $n = 7$, compositions with strontium contents slightly higher than those used for the synthesis of the orthorhombic phase. A mixture of two phases was observed by X-ray powder diffraction for these compositons; an example is given in Table I for a nominal cation ratio of 13.2/21.9/13. The peaks attributed to the second phase (stared) do not correspond to any phase of the Bi–Sr–Cu–O system.

The electron diffraction study showed the coexistence of two sorts of grains: the orthorhombic tubular-7 phase and a new monoclinic phase which is the purpose of this study. Up to now, it was not possible to isolate this compound so that its actual composition cannot be given with accuracy. Never-

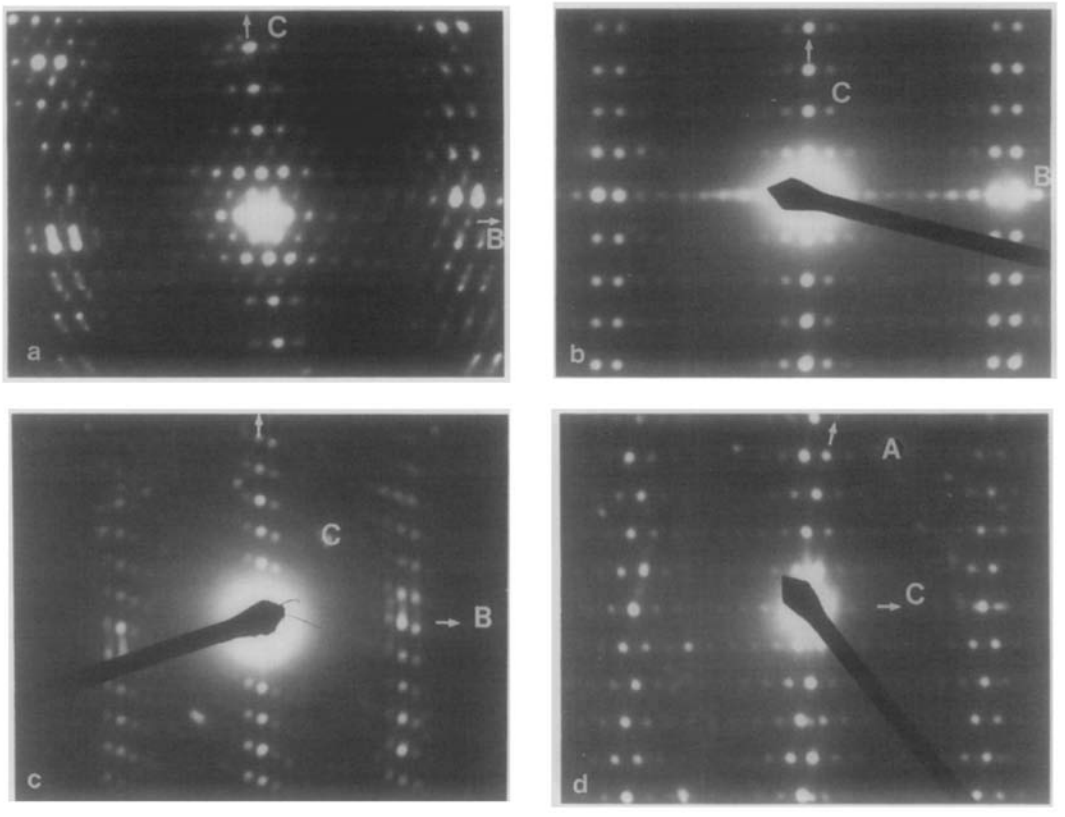

FIG. 2. Corresponding electron diffraction patterns of (a) monoclinic new phase, (b) orthorhombic tubular $n = 7$ phase, (c) monoclinic modulated 2201 superconductor, and (d) monoclinic "collapsed" phase.

theless, the electron microscopy study shows that it is closely related to the orthorhombic form, suggesting that its composition is close to that of the orthorhombic phase.

Electron Diffraction Study

The electron diffraction investigation of this new phase allowed its monoclinic cell to be determined:

$$a \approx a_p\sqrt{2} \approx 5.4 \text{ Å}, b \approx 24.7 \text{ Å}, c \approx 24.65 \text{ Å}, \alpha \approx 96°.$$

The examination of the [100] E.D. patterns of this phase (Fig. 2a) and of the orthorhombic tubular-7 oxide (Fig. 2b) shows their great similarity. The intense spots of the two phases exhibit a similar distribution. Indeed, a sequence of $(n + 1)$ weak spots and two intense dots was observed along the B_n axis of a member "n" of the orthorhombic tubular phase (3). In the monoclinic phase the modulation is 16 weak spots and two intense ones.

The extra reflections of the X-ray pattern (Table I) can be indexed taking into account this monoclinic cell; it should be noted that $hk0$ and $h0l$ reflections of the orthorhombic and monoclinic phases are overlapped. The E.D. patterns show that the spots of the monoclinic phase exhibit a systematic arcing, correlated to the existence of slightly misoriented domains (Fig. 2a and Fig. 3).

TABLE I

OBSERVED AND CALCULATED X-RAY DIFFRACTION PATTERN

d_{obs} (Å)	d_{calc} (Å)	*hkl* (ortho)	I/I_0	Extra reflections[a]
12.3	12.265	002	22	
5.288	5.281	101	5	
4.086	4.117	060	21	
	4.088	006		
3.862	3.881	026	4	
	3.847	054		
3.745	—	—	7	$(14\bar{3})$
3.643	3.642	143	19	
3.546	—	—	15	(143)
3.325	3.331	153	70	
	3.324	135		
3.228	—	—	10	$(153)(14\bar{5})$
3.134	3.132	145	22	
3.089	3.088	080	33	
3.072	3.063	008		
3.047	3.043	018	35	$(15\bar{5})(145)$
	3.041	163		
3.003	2.994	082	9	
2.948	2.941	107	100	
2.932	2.934	171		
	2.927	155		
2.894	2.900	066	5	
2.833	—	—	11	(155)
2.709	2.714	165	81	
2.704	2.704	200		
2.649	2.655	147		
2.644	2.641	220	20	
	2.641	202		
2.530	2.531	175	1	
	2.527	157		
2.470	2.470	0 10 0	22	
2.454	2.453	0 0 10	26	

[a] The orthorhombic cell was indexed on the bases of the following parameters: $a = 5.408$ Å; $b = 24.70$ Å, and $c = 24.53$ Å. Stars indicate the reflections unindexed in the orthorhombic cell; they can be indexed in a monoclinic cell deduced from the orthorhombic cell with $\alpha \approx 96°$.

The comparison of these E.D. patterns with the [100] E.D. pattern of the superconducting 2201 oxide (Fig. 2c) and the [010] E.D. pattern of the monoclinic collapsed 2201 phase (Fig. 2d) suggests that these four phases exhibit close structural relationships. The superconducting 2201 oxide (Fig. 2c) differs from the other phases by the existence of incommensurate satellites; the amplitude and the angle of the modulation vector vary with the cationic composition (*9*), implying an evolution from a monoclinic to an orthorhombic super cell.

HREM Study: A Structural Model of the Monoclinic Phase $(Bi_2Sr_2CuO_6)_n \cdot Sr_8Cu_6O_{16+y}$

In order to understand the mechanism which presides to the formation of the monoclinic phase, high resolution images have been recorded. The [010] image of this phase (Fig. 3) shows that the "brick wall"-like contrast characteristic of the orthorhombic tubular-7 phase (*3*), arising from the existence of the double BiO layers and the perovskite-related slice, is also observed here. However, it appears clearly that the white dots correlated to the $[Sr_8Cu_6O_{16}]_\infty$ perovskite slice do not build up a "pillar" perpendicular to the bismuth layers any more but form oblique lines, with an angle close to 96°. The analysis of the enlarged images (Fig. 4) gives evidence of the coexistence of two types of structural units:

—orthorhombic-tubular members similar to those previously observed;

—monoclinic-tubular members which can be deduced from the orthorhombic one by translating a copper layer of about 2.7 Å along **b**. If such a displacement was regularly applied to the copper layers, it would lead to the schematized model of Fig. 5b, which shows that the main difference with the orthorhombic form (Fig. 5a) deals with the nature of the $[Sr_8Cu_6O_{16}]_\infty$ perovskite-like slices which do not exhibit corner sharing CuO_6 octahedra but double rows of corner sharing CuO_4 tetrahedra and CuO_5 bipyramids running along **a**. The theoretical parameters of such a monoclinic cell are

$$a_m \approx a_n \approx a_p\sqrt{2},$$
$$b_m \cong b_n,$$
$$c_m \approx \frac{c_n}{2 \sin \alpha},$$
$$\text{and } \alpha \approx 102°5 \left(\text{tg}\,(\alpha - 90°) = \frac{a_p\sqrt{2}}{c_n} \right),$$

where m, n, and p are referred to the monoclinic cell, the orthorhombic tubular-n cell, and the ideal perovskite cell, respectively.

The way these two structural units are

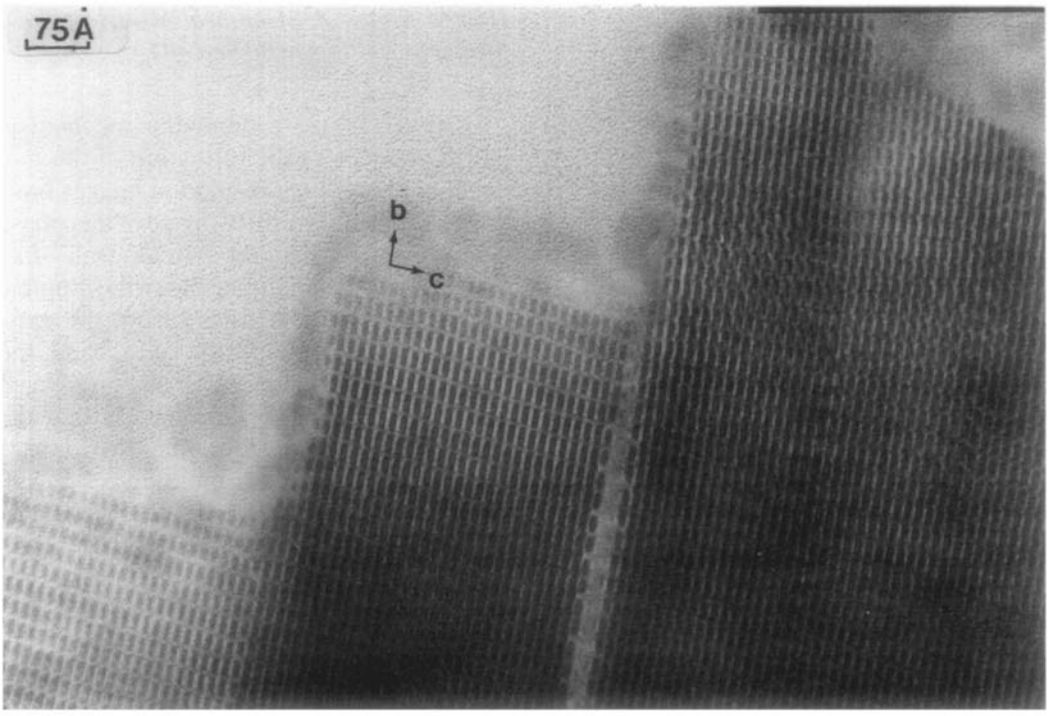

FIG. 3. [100] image of the new monoclinic phase showing the "brick-wall"-like contrast and the existence of numerous domains.

arranged can be deduced from the image (Fig. 4), taking into account the width of the rectangles, characteristic of the n value, and the relative disposition of the squares of the $[Sr_8Cu_6O_{16}]$ slices, defined by four Sr–Cu–Sr segments and located in the copper layers on both sides of the $[BiO]_2$ layers. This is illustrated in Fig. 6a, and the two different possible dispositions of the squares are schematically drawn in Fig. 6b, where

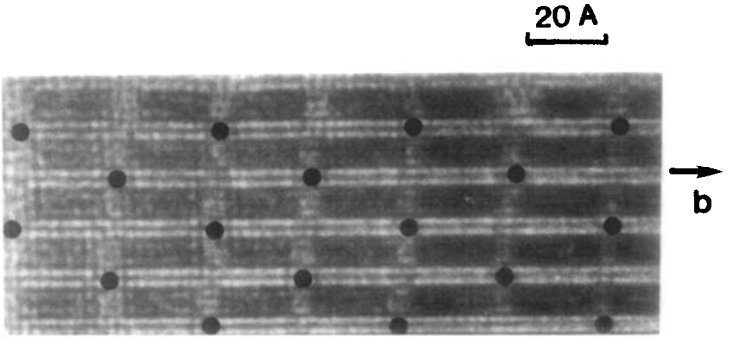

FIG. 4. Enlargement of a [100] image of the monoclinic phase. Black dots indicate the presence of an orthorhombic member (see Fig. 6).

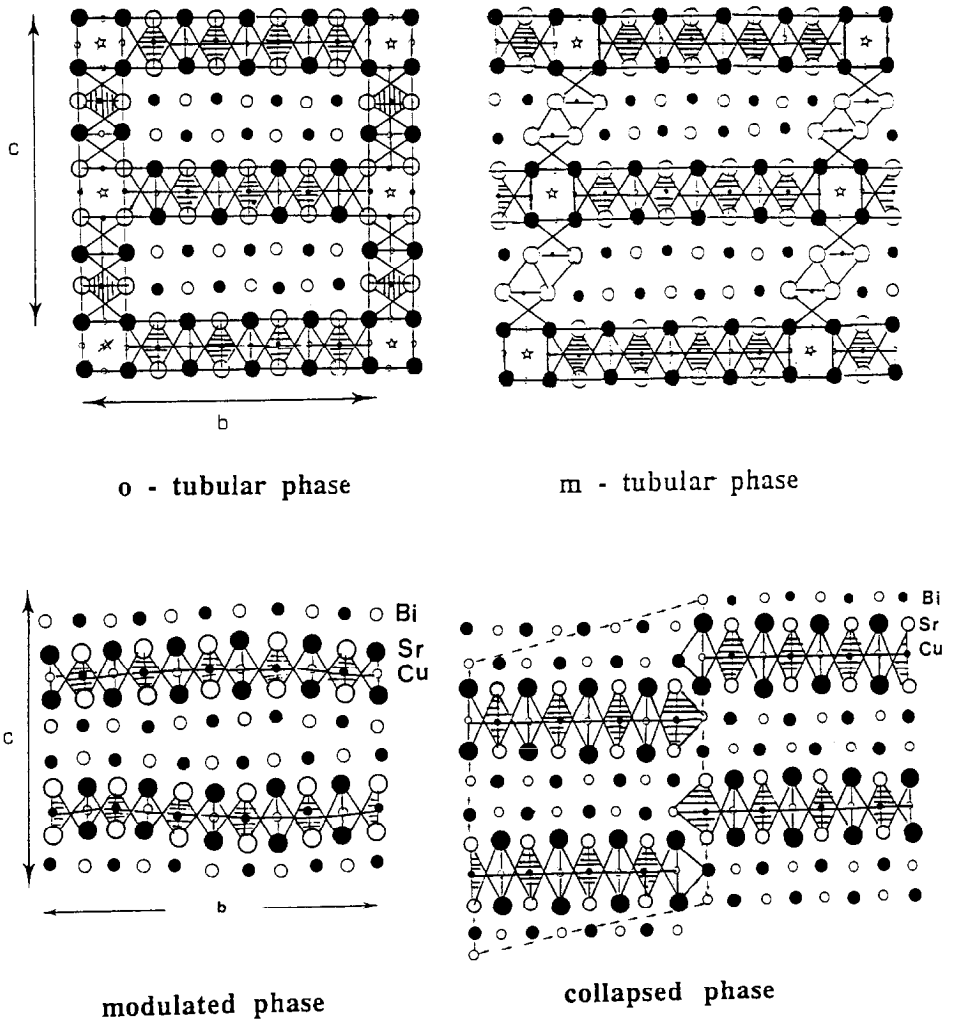

FIG. 5. Idealized drawing of the "2201"-related phases: (a) orthorhombic $n = 7$ tubular phase; (b) monoclinic $n = 7$ tubular phase; (c) 2201 modulated phase, superconducting; and (d) monoclinic "collapsed" phase (according to (9)).

the double bismuth layers are represented by two black lines and the [Sr–Cu–Sr] squares in the copper layers by squares; a black dot indicates that the two squares are aligned along **c** in the orthorhombic phase whereas they are shifted $a_p\ \sqrt{2}/2$ in the monoclinic phase.

In the new phase, it appears that monoclinic and orthorhombic units regularly alternate along the **b** and **c** axes, as shown in Fig. 6a. Such a double mechanism implies that starting from an $n = 7$ layer the adjacent layer is built up from $n = 6$ and $n = 8$ members owing to the shifting of the pillar. The third layer is again built up from $n = 7$ members and so on. In that way, slices of $n = 7$ members alternate with slices of $n = 6 + n = 8$ members, the average composition $n = 7$ being kept up. The idealized drawing of the model is shown in Fig. 6c.

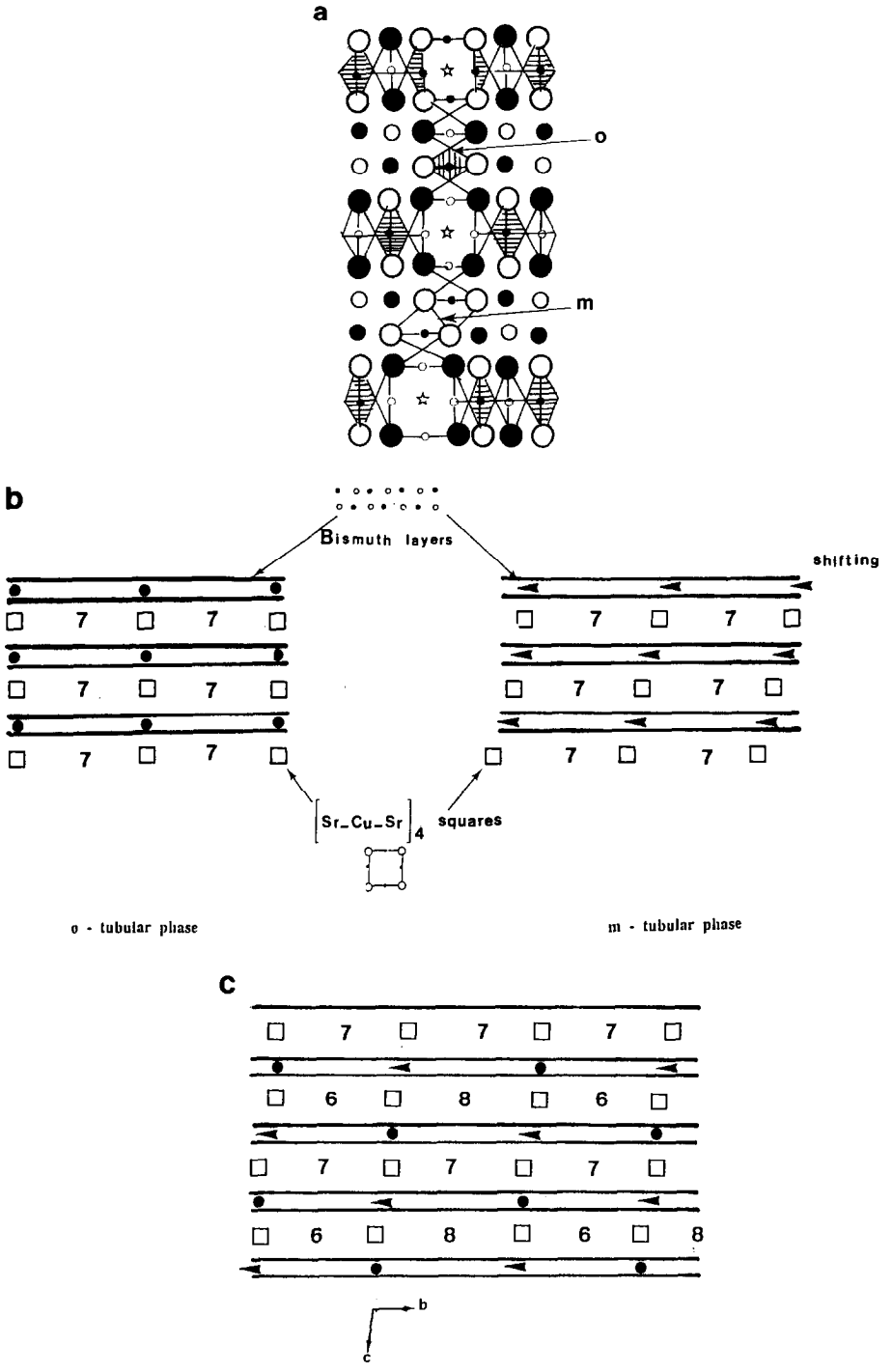

FIG. 6. (a) Alternance of the orthorhombic (*o*) and monoclinic (*m*) units at the level of the perovskite layers. (b) Schematic drawing of the two forms of the tubular phases. The "bismuth" layers are represented as black lines, the squares defined by Sr–Cu–Sr segments as open squares. The shifting of the Bi/Sr layers is represented by a black arrow (see Fig. 7) and the orthorhombic arrangement by black dots. (c) Schematic representation of the enlarged image in Fig. 4. A double intergrowth of *o* and *m* members is observed simultaneously along **b** and **c**. Combining *o* and *m* mechanisms implies the alternance of $n = 7$ slabs and mixed $n = 6$ and $n = 8$ slabs. The average composition is $n = 7$.

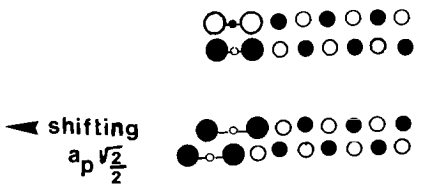

FIG. 7. Representation of the shifting $a_p\sqrt{2}/2$ of the Sr–Cu–Sr segments at the level of the "bismuth" layers.

The real composition of the new monoclinic phase can be rather formulated as $[(Bi_2Sr_2CuO_6)_7]_2$ $(Bi_2Sr_2CuO_6)_6$ $(Bi_2Sr_2CuO_6)_8$ $(Sr_8Cu_6O_{16+y})_4$ and the theoretical parameters are:

$$a \approx a_p\sqrt{2}$$
$$b \approx 2 \times b_7 \approx b_6 + b_8$$
$$\approx \left[\left(8 \times \frac{a_p\sqrt{2}}{2}\right) + a_p\right] \times 2$$
$$c \approx c_7(\sin\alpha)^{-1},\ \alpha \approx 96°$$
$$\mathrm{tg}(\alpha - 90°) = \frac{a_p\sqrt{2}}{2.c_7}.$$

This shearing phenomenon between two successive copper layers can be compared to those observed for the 2201 phases. First, the structure of the monoclinic collapsed 2201 oxide (Fig. 5d) can be deduced from that of the pseudo-orthorhombic 2201 modulated oxide (Fig. 5c) by a similar rupture between two neighboring CuO_6 octahedra. However, in the latter case the shifting is of about 3.9 Å and takes place in the direction perpendicular to the copper layers, leading to the formation of zig-zag distorted rock salt layers running along **b**, the copper layers being interrupted and replaced by BiO layers (Fig. 5d). Second, let us consider the (Bi/Sr)O layers of the tubular-7 phase; they consist of quadruple "O–Bi–O–Bi–O–Bi–O–Bi–O" and triple "O–Bi–O–Bi–O–Bi–O" strings running along **b** separated by "O–Cu–O" and "Sr–O–Sr" segments (Fig. 7) leading to a mean cationic composition "Bi_7Sr_2Cu" for one (Bi/Sr)O layer. In the orthorhombic tubular phase the "Sr–Cu–Sr" segments are located at the same level along **b** in the bismuth layers (Fig. 6a), whereas they are shifted by 2.7 Å in the monoclinic form (Fig. 6b). Such a shifting of the bismuth layers can be compared to that observed in the superconducting modulated phases 2201 and 2212, which involves, in the same way, orthorhombic or monoclinic supercells (*15*).

Orthorhombic and Monoclinic Intergrowths

In some part of the crystals, different arrangements of the two structural units are observed. An example is shown in Fig. 8a. It can be seen that one orthorhombic member (black dots) alternates with two monoclinic members simultaneously along the **b** and the **c** axes; only one double intergrowth is observed in that area (on the diagonal of the image). The angle α of the monoclinic cell is locally greater (≈98.5°) and the parameters b and c multiplied by $\frac{2}{3}$; one slab of members $n = 7$ is stacked with two mixed slabs of "$(n = 6) + (n = 7) + (n = 8)$" owing to the mechanism of shifting, as shown in the schematic model in Fig. 8b. The average composition remains equal to $n = 7$.

It should be noted that the overall number of monoclinic members are almost equal to that of the orthorhombic ones in the "monoclinic" crystals, leading to an average α angle close to 96° (Fig. 4) and a mean composition close to that of the $n = 7$ members.

It can be seen that in such intergrowth of monoclinic and orthorhombic structures every member, m or o, are aligned along the [011] direction of the orthorhombic $n = 7$ cell (white arrows).

Disordered Sequences of n Members

As in most of the phases built up from the intergrowth of two structural units, the existence of aleatory sequences is ob-

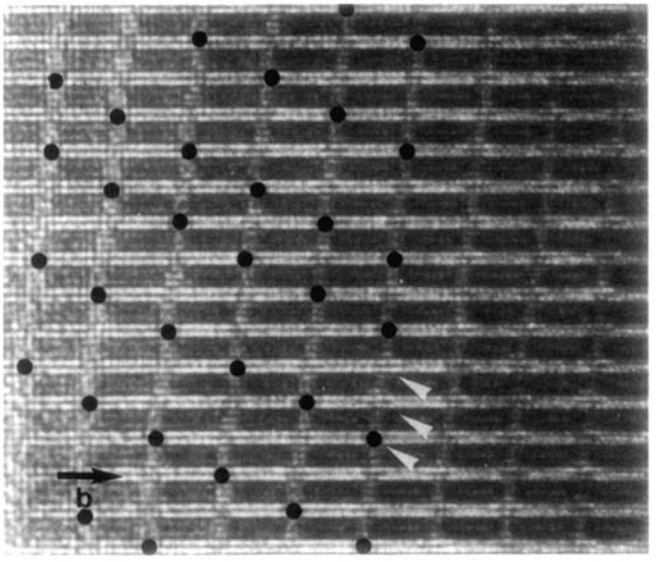

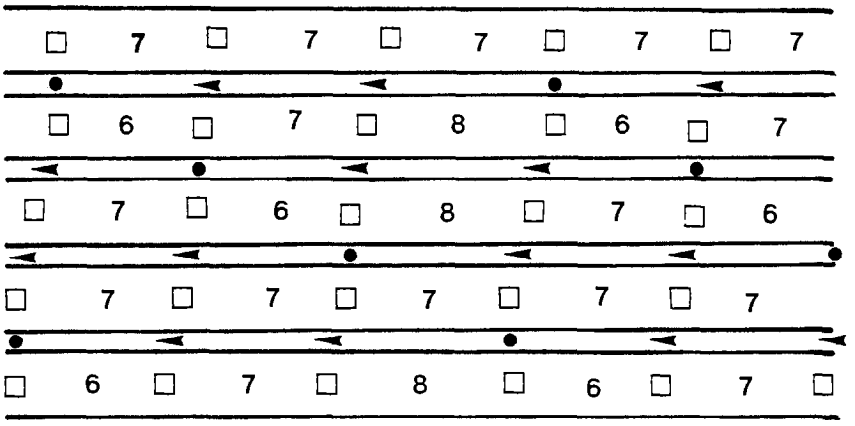

FIG. 8. (a) [100] enlarged image of a different arrangement of the orthorhombic (black dots) and monoclinic units. It consists in a triple intergrowth of one orthorhombic and two monoclinic units along **b** and **c** simultaneously. (b) Schematic drawing of the disposition of the different members. One $n = 7$ slab alternates with two mixed $n = 6 + n = 7 + n = 8$ slab. The average composition is $n = 7$.

served when the n value increases in the tubular phases (*3*). The images of defective crystals show that the variation of the n value from one member to the adjacent is observed as well along **b** as along **c** (Fig. 9). These highly disordered phases correspond, in fact, to the phase labeled "D" by Matsui *et al.* (*16*).

This implies that the $[Sr_8Cu_6O_{16}]_\infty$ pillar has been shifted along **b** from one slice to the adjacent one in the same way as in the monoclinic tubular phase. In such defective

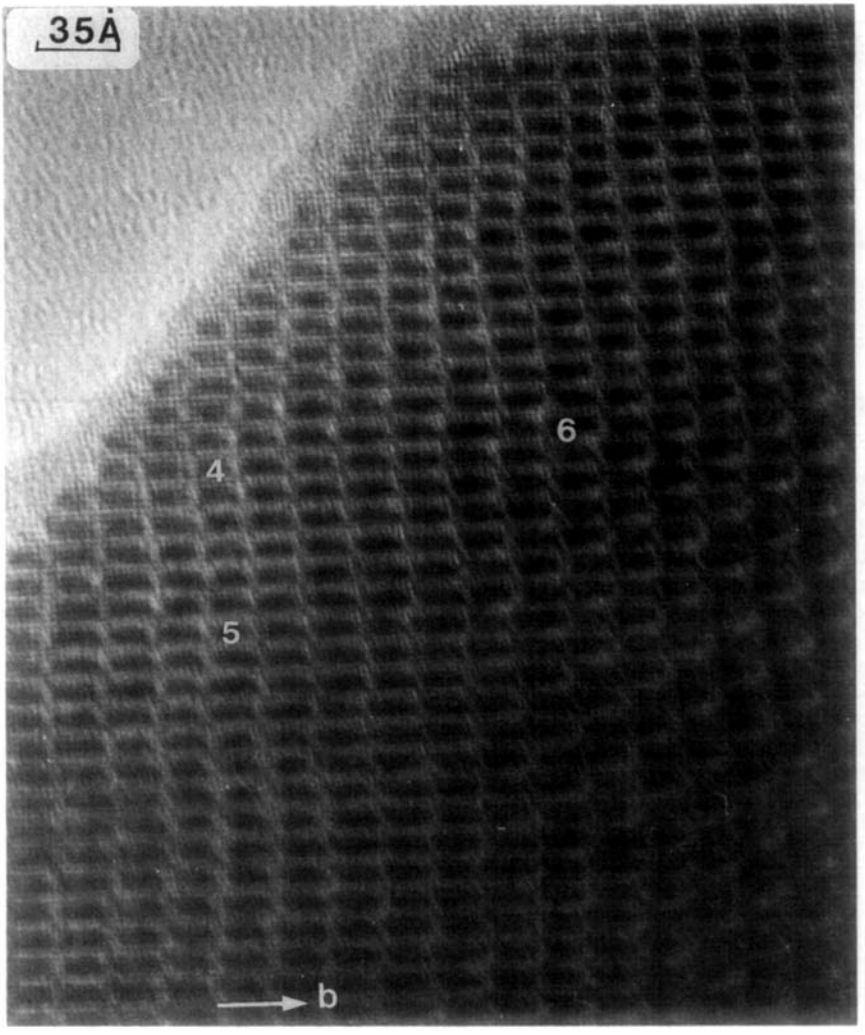

FIG. 9. Typical [100] image of aleatory sequences of orthorhombic and monoclinic members. They are observed in samples of nominal compositions corresponding to $n > 7$ and noninteger n values.

crystals the "Sr–Cu–Sr" units undulate along the **c** axis.

Conclusion

The monoclinic tubular phase, obtained for small variations of cationic molar ratios with regard to the nominal composition of the orthorhombic tubular $n = 7$ phase, results from an intergrowth mechanism. It corresponds indeed to a double intergrowth along the **b** and the **c** axes of orthorhombic members and monoclinic members whose structure can be described by a shifting of one $[(Bi, Sr)O]_\infty$ layer along **b**, $(a_p \sqrt{2}/2)$, with regard to the adjacent one, simultaneously with a shearing of the $[Sr_2Cu]_4$ squares. These mechanisms are similar to those observed in the modulated 2201 superconducting oxides, which generate either the ortho-

rhombic and monoclinic modulated supercells and the monoclinic collapsed phase. The same structural mechanism is involved in the formation of the disordered crystals obtained for the high n values of the tubular phases.

Acknowledgments

M. Caldes and A. Fuertes acknowledge the Spanish CICYT (Grants MAT 88-0/63-603 and MAT 90-1020-602-01) and the MIDAS program for support of this research.

References

1. A. Fuertes, C. Miratvilles, J. Gonzalez-Calbet, M. Vallet-Regi, X. Obradors, and J. Rodriguez-Carjaval, *Physica C* **157,** 529 (1989).
2. M. T. Caldes, J. M. Navarro, F. Perez, M. Carrera, J. Fonteuberta, N. Casan-Pastor, C. Miratvilles, X. Obradors, J. Rodriguez-Carjaval, J. M. Gonzales-Calbet, M. Vallet-Regi, A. Garcia, and A. Fuertes, Chemistry of Materials, in press.
3. M. T. Caldes, M. Hervieu, A. Fuertes, and B. Raveau, *J. Solid State Chem.*, in press.
4. C. Michel, M. Hervieu, M. M. Borel, A. Grandin, F. Deslandes, J. Provost, and B. Raveau, *Z. Phys. B: Condens. Matter* **68,** 421 (1987).
5. J. B. Torrance, Y. Tokura, S. J. La Placa, T. C. Huang, R. J. Savoy, and A. I. Nazzal, *Solid State Commun.* **66,** 703 (1988).
6. R. S. Roth, *in* "Proceedings, Am. Phys. Soc. Meeting, New Orleans, March 1988."
7. A. K. Cheetham, A. M. Chippindala, and S. J. Hibble, *Nature* **333,** 21 (1988).
8. R. S. Roth, C. J. Rawn, and I. A. Bendersky, *J. Mater. Res.* **5,** 46 (1990).
9. Z. Hiroi, Y. Ikeda, M. Takano, and Y. Bando, *J. Mater. Res.* **6,** 435, 1991.
10. Y. Ikada, H. Ito, S. Shimomura, Y. Ore, K. Inaba, Z. Iroi, and M. Takano, *Physica C* **157,** 93 (1989).
11. R. S. Roth, C. J. Rawn, B. P. Burton, and F. Beech, *J. Res. Nat. Inst. Stand. Technol.* **95**(3), 291 (1990).
12. A. Saggio, K. Sugata, J. Hahn, S. J. Mwu, D. R. Poeppelmeir, and T. O. Mason, *J. Am. Ceram. Soc. Commun.* **72,** 849 (1989).
13. B. C. Chakoumakos, P. S. Ebey, B. C. Sales, and E. Sonders, *J. Mater. Res.* **4,** 767 (1991).
14. J. A. Saggio, K. Siyata, J. Hahn, S. J. Hwu, K. Poeppelmeier, and T. O. Mason, *J. Am. Ceram. Soc.* **72,** 849, 1989.
15. H. W. Zandbergen, W. A. Groen, F. C. Mijlhoff, G. Van Tendeloo, and S. Amelinckx, *Physica C* **156,** 325 (1988).
16. Y. Matsui, S. Takekawa, H. Nozaki, and A. Umezono, *Jpn. J. Appl. Phys.* **28,** L602 (1989).